Application of Schrödinger Equation to Study the Tunnelling Dynamics of Proton Transfer in the Hydrogen Bond of 2,5-Dinitrobenzoic Acid: Proton T_1, $T_{1\rho}$, and Deuteron T_1 Relaxation Methods

L. Latanowicz*,† and W. Medycki‡

Institute of Biotechnology and Environmental Sciences, University of Zielona Góra, Szafrana 1, 65-516 Zielona Góra, Poland, Institute of Molecular Physics, Polish Academy of Science, Smoluchowskiego 17, 60-179, Poznań, Poland

Received: July 28, 2006; In Final Form: October 28, 2006

Temperature measurements of proton T_1 (24.7 MHz), deuteron (deuterated hydroxyl group) T_1 (55.2 MHz), and proton $T_{1\rho}$ ($B_1 = 9$ G) spin−lattice relaxation times of 2,5-dinitrobenzoic acid have been performed. An analysis of present experimental data together with previously published proton T_1 (55.2 MHz) data has revealed the following molecular motions: proton/deuteron transfer in the hydrogen bond and two-site hopping of the whole dimer. It is shown that the proton-transfer dynamics are characterized by two correlation times τ^{ov} and τ^{tu}, describing two fundamentally different motional processes, namely, thermally activated jumps over the barrier and tunneling through the barrier. The temperature dependence of $1/\tau^{tu}$ is the solution of Schrödinger's equation, which also yields the temperature T_{tun}, where begins the tunnel pathway for proton transfer. A new equation for the spectral density function of complex motion consisting of the three motions is derived. The third motion (two-site hopping of the whole dimer characterized by τ^{lib} correlation time) is responsible for a proton $T_{1\rho}$ minimum in high temperatures, just below the melting point. Such a minimum is not reached by T_1 temperature dependencies. The minimum of $T_{1\rho}$ assigned to the classical hopping of a hydrogen-bonded proton occurs in the same low-temperature regime in which the flattening of the temperature dependencies of T_1 points to the dominance of incoherent tunneling. This experimental fact denies the known theories predicting the intermediate temperature regime where a smooth transition between classical and quantum tunneling dynamics is expected. The fit of the derived theoretical equations to the experimental data $T_{1\rho}$ and T_1 is satisfactory. The correlation times obtained for deuterons indicate deuteron-transfer dynamics much slower than proton-transfer dynamics. It is concluded that the classical proton transfer takes place over the whole temperature regime, while the incoherent tunneling occurs below 46.5 (hydrogen) or 87.2 K (deuterium) only.

1. Introduction

The purpose of this paper is to study of the proton-transfer dynamics of 2,5-dinitrobenzoic acid (2,5-DNBA) in a wide temperature regime by the NMR relaxation method. The measurements of proton relaxation were performed at high [T_1 (24.7 MHz)] and low [$T_{1\rho}$ ($B_1 = 9$ G)] resonance frequencies. The deuteron T_1 (55.2 MHz) relaxation for 2,5-DNBA, deuterated in the mobile proton places (OD groups) was also measured. The proton T_1 (55.2 MHz) measurements were published previously.[1]

Proton/deuteron transfer in the hydrogen bonds of carboxylic acid dimers is a stochastic process, which modulates the interaction Hamiltonian; therefore, it can be studied using NMR relaxation methods. The assumption that the proton/deuteron transfer is a single stochastic process (characterized by single correlation time) with a smooth transition from the classical (at high temperatures) to quantum dynamics (at low temperatures) of proton transfer in the intermediate temperature regime has been made in a number of papers.[1−13]

At variance to the above point of view, a new theoretical description of the proton transfer as a complex motion has been proposed in refs 14−16. The complex motion means that the proton/deuteron transfer consists of two independent, constituent motions, namely, classical hopping over the barrier and incoherent tunneling through the barrier between sites corresponding to potential energy minima (Figure 1). Since both motions take place between the same potential minima, the geometries of these motions are identical. These motions characterized by the correlation times τ^{ov} (thermally activated jumps over the barrier, classical motion) and τ^{tu} (incoherent tunneling) contribute to separate correlation functions. As follows from the Schrödinger equation, the tunnel jumps take place only when the potential barrier is transparent for the de Broglie'a wave.[16] The total spectral density of complex motion is a Fourier transform of the total autocorrelation function which is a product of the separate correlation functions.[17]

The temperature dependence of the correlation time of thermally activated jumps over the barrier τ^{ov} follows the Arrhenius law:

$$\tau^{ov} = \frac{1}{(1+a)}\,\tau_0^{ov}\exp\left(\frac{E_{ov}}{RT}\right) \qquad (1)$$

where

* Author to whom correspondence should be addressed. Tel.: 48-61-6639787. Fax: 48-61-8798202. E-mail: jlat@amu.edu.pl.
† University of Zielona Góra.
‡ Polish Academy of Science.

10.1021/jp0648442 CCC: $37.00
Published on Web 01/31/2007

$$a = \exp\left(\frac{\Delta}{RT}\right) \tag{2}$$

and $E_{ov} = E_{AB}$ is the activation energy (barrier height minus the energy of the ground vibrational state) of Avogadro's number of objects, T is the temperature in Kelvin, τ_0^{ov} is the pre-exponential factor, and Δ is the energy difference between the potential minima ($\Delta = E_{AB} - E_{BA}$). The Arrhenius law does not predict some final temperature for the application of eq 1, but at the very low temperatures, the values of τ^{ov} are too long to give the perceptible contribution of the corresponding spectral density to the spin−lattice relaxation at the megahertz resonance frequencies (T_1). The best detection of τ^{ov} correlation time at low temperatures is the spin−lattice relaxation rate measured at a low resonance frequency in the kilohertz range, that is, ($1/T_{1\rho}$).

Skinner and Trommsdorff[2] and Nagaoka et al.[18] have derived equations for the correlation time of incoherent tunneling. The temperature limitations of τ^{tu} are not expected from these formulas.

The correlation time of incoherent tunneling following from the Schrödinger equation has been proposed in refs 19−21:

$$\tau^{tu} = \tau_0^{tu} \exp[B\sqrt{(E_{ov} - C_pT)}] \tag{3}$$

where

$$B = \frac{2L}{\hbar}\sqrt{\frac{2m}{N_{Av}}} \tag{4}$$

The value of B in eq 4 depends on the mass m of the tunneling particle and on the width L of the potential barrier. The masses of the tunneling proton and deuteron, m, are 1.67×10^{-27} and 3.346×10^{-27} kg, respectively. The width of the potential barrier, L, which can be estimated from the crystallographic data[22] is $L = 0.71$ Å (the distance between protons from two tautomeric forms O−H···O ↔ O···H−O). Thus, the values of B are then found to be 0.1006 $(\sqrt{J})^{-1}$ for the proton and 0.142 $(\sqrt{J})^{-1}$ for the deuteron. C_p is the molar specific heat.

The Schrödinger equation predicts that the tunnel jumps through the potential barrier appear when the energy of the particle is lower than the value of the potential barrier that the particle has to pass over. The energy of the particle is the sum of the thermal energy decreasing with decreasing temperature and the vibrational energy; so for 1 mole of molecules, $E = C_pT + E_{v0}$, where C_p is the molar heat capacity and E_{v0} is the vibrational energy. The height of the barrier V is the activation energy plus the vibrational energy $V = E_{ov} + E_{v0}$; so, the tunnel jumps occur in temperatures meeting the condition $C_pT < E_{ov}$. The problem of the absence of correlation functions of incoherent tunneling at high temperatures has been discussed in the literature.[15,16,19−21]

The proton transfer in a hydrogen bond is not the only motion which governs the total spectral density function. The minimum of proton $T_{1\rho}$, which can be assigned to librations of the whole dimer (Figure 1), is observed for 2,5-DNBA at high temperatures. The correlation time characterizing this motion can be defined as

$$\tau^{lib} = \tau_0^{lib} \exp\left(\frac{E_{lib}}{RT}\right) \tag{5}$$

where E_{lib} is the activation energy of this motion and τ_0^{lib} is the pre-exponential factor.

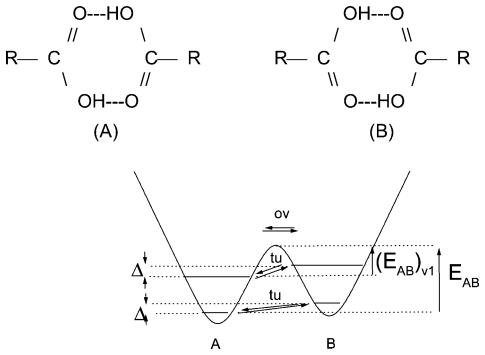

Figure 1. A and B tautomers of carboxylic acid dimer and the corresponding potential energy minima. $v0$ and $v1$ are local vibrational states.

Thus, the three stochastic processes—classical and quantum-mechanical proton jumps in the hydrogen bond and librations of the whole dimer between two equilibrium positions—independently modulate the interaction Hamiltonian. The expression describing the spectral density function of the complex motion consisting of the three motions is derived in this paper and applied to analyze the proton and deuteron T_1 and also proton $T_{1\rho}$ temperature dependencies in 2,5-dinitrobenzoic acid. Such an analysis cannot be performed in terms of the known equations for the spectral density of proton transfer. It will be shown that it is not possible to obtain an acceptable fit to the $T_{1\rho}$ data by employing these known equations.

2. The Theory of Spin−Lattice Relaxation

In the case of proton spin−lattice relaxation, the average value of all dipolar interactions has to be taken into account. Since the whole molecules obey the Boltzmann distribution between vibrational levels (a vibrational relaxation is much faster than T_1 relaxation), the relaxation rate is given by

$$\frac{1}{(T_1)} = \frac{1}{N}\sum_{i=1}^{N}\sum_{s=1}^{N}\left(n_{v0}\frac{1}{(T_1^{is})_{v0}} + n_{v1}\frac{1}{(T_1^{is})_{v1}}\right) \tag{6}$$

where N is the number of protons in a molecule; n_{v0} and n_{v1} are the Boltzmann fractions of molecules in the separate vibrational levels $v0$ and $v1$ associated with the average energies E_{v0} and E_{v1} of the ground and first excited vibrational levels. Because the population of molecules in the second excited vibrational level is very low, it seems reasonable to take into account only two vibrational levels [$n_{v0} + n_{v1} = 1$, $n_{v1}/n_{v0} = \exp(-\delta E_{v01}/\mathrm{RT})$, where $\delta E_{v01} = E_{v1} - E_{v0}$ is the energy difference between the ground and first exited vibrational states]. Therefore, the values of n_{v0} and n_{v1} are

$$n_{v0} = \frac{\exp(\delta E_{v01}/RT)}{\exp(\delta E_{v01}/RT) + 1} \tag{7}$$

and

$$n_{v1} = \frac{1}{\exp(\delta E_{v01}/RT) + 1} \tag{8}$$

In the weak-collision limit, the spin−lattice relaxation rates in the laboratory and rotating frames for the standard type of spin interactions, such as the direct dipole−dipole interaction of homonuclear spin pair *is*, are given by[23−25]

$$\frac{1}{(T_1^{is})_{\upsilon x}} = \frac{9}{8}\left(\frac{\mu_0}{4\pi}\right)^2 [J_{is}{}^1(\omega_I) + J_{is}{}^2(2\omega_I)] \quad (9)$$

and

$$\frac{1}{(T_{1\rho}^{is})_{\upsilon x}} = \frac{9}{8}\left(\frac{\mu_0}{4\pi}\right)^2 \left[\frac{1}{4} J_{is}{}^0(2\omega_1) + \frac{5}{2} J_{is}{}^1(\omega_I) + \frac{1}{4} J_{is}{}^2(2\omega_I)\right] \quad (10)$$

The quadrupolar interaction of the deuteron spins can be described in terms of the single-spin quadrupolar coupling tensor. The largest tensor component qcc_{zz} is normally aligned parallel to the chemical bond. The spin−lattice relaxation of a nuclear spin I with a quadrupole moment resulting from the time-dependent fluctuations of the electric field gradient at the nucleus can be expressed as[26−28]

$$\frac{1}{(T_1^{\text{deut}})_{\upsilon x}} = \frac{9}{8}\left(\frac{\mu_0}{4\pi}\right)^2 \left(1 + \frac{\eta^2}{3}\right)\pi^2 [J_{qcc}{}^1(\omega_I) + J_{qcc}{}^2(2\omega_I)] \quad (11)$$

where $\upsilon x = \upsilon 0$ and $\upsilon x = \upsilon 1$; η is the asymmetry parameter. The angular NMR frequency in the laboratory frame is ω_I, while $\omega_1 = \gamma_I B_1$ is the frequency of the rotating magnetic field and $J_{is}^m(2\omega_1)$, $J_{is(qcc)}^m(\omega_I)$, and $J_{is(qcc)}^m(2\omega_I)$ where $m = 0$, 1, and 2 are the spectral density functions of the correlation functions of the fluctuating part of the dipolar or quadrupolar Hamiltonian. These random functions are

$$F^0(t) = L(t)\,\{1 - 3\cos^2[\vartheta(t)]\} \quad (12)$$

$$F^1(t) = L(t)\,\{\sin[\vartheta(t)]\cos[\vartheta(t)]\exp[i\varphi(t)]\} \quad (13)$$

$$F^2(t) = L(t)\,\{\sin^2[\vartheta(t)]\exp[2i\varphi(t)]\} \quad (14)$$

The quantity $L(t)$ in eqs 9−11 equals $\gamma_i\gamma_s\hbar\, R_{is}{}^{-3}(t)$, which is the dipole coupling constant, or $L(t) = e^2\, q_{zz}(t)\, Q/h$, which is the quadrupole coupling constant expressed in hertz. The polar and azimuth angles $\vartheta(t)$ and $\varphi(t)$ describe the orientation of R_{is} or q_{zz} in the laboratory frame with the z axis in the direction of the external magnetic field B_0. The parameters q_{zz}, R_{is}, ϑ, and φ are time-dependent.

The proton NMR relaxation monitors the dynamics of two protons at a distance R_{is}, while the deuteron relaxation monitors the dynamics of the X−D chemical bond. The sources of the differences in the spectral densities for $\upsilon 0$ and $\upsilon 1$ levels are the different potential barriers for the classical jumps [$(E_{AB})_{\upsilon 1} = E_{AB} - \delta E_{\upsilon 01}$ and $(E_{BA})_{\upsilon 1} = E_{AB} - \Delta - \delta E_{\upsilon 01}$ (Figure 1)] and also different frequencies of the tunneling jumps [$(1/\tau_0^{tu})_{\upsilon 1} \approx 1/30(\tau_0^{tu})_{\upsilon 0}$].[8] As the spectral densities $J_{is(qcc)}^m(\omega)$ depend on the fluctuations of the dipolar or quadrupolar Hamiltonian, the results presented in this paper imply the need to derive a formula for the correlation function of a complex motion composed of three components. Two components are the classical hopping (jumps over the barrier) and incoherent tunneling (jumps through the barrier) between two sites A and B of unequal energy (Figure 1). The third component describes the jumps over the barrier of R_{is} or q_{zz} between two equilibrium sites of equal energy. One set of sites is distanced by the Θ_{AB} angle and E_{AB} potential barrier and the second one is distanced by the Θ_{lib} angle and E_{lib} activation energy.

When the method for the correlation function calculation presented in ref 14 is applied, derivation of the formula for the complex motion is easy:

$$\langle F^m(t)\, F^m{}^*(t+t)\rangle_{\upsilon x} = \frac{S^m}{(C_1 + C_2)}\left[C_1 + C_2\exp\left(-\frac{|\tau|}{\tau_{\upsilon x}^{ov}}\right)\right]\left[\left(C_1 + C_2\exp\left(-\frac{|\tau|}{\tau_{\upsilon x}^{tu}}\right)\right)\right] \times \left[1 - \frac{3}{4}\sin^2(\Theta_{lib}) + \frac{3}{4}\sin^2(\Theta_{lib})\exp\left(-\frac{|\tau|}{\tau^{lib}}\right)\right] \quad (15)$$

where

$$C_1 = \frac{a}{(a+1)^2}\left[aL(A)^2 + \frac{1}{a}L(B)^2 + L(A)L(B)(3\cos^2\Theta_{AB} - 1)\right] \quad (16)$$

and

$$C_2 = \frac{a}{(a+1)^2}[L(A)^2 + L(B)^2 - L(A)L(B)(3\cos^2\Theta_{AB} - 1)] \quad (17)$$

where "a" is given by eq 2. The parameters $\tau_{\upsilon x}^{ov}$, $\tau_{\upsilon x}^{tu}$, and τ^{lib} are the correlation times characterizing the separate motions. $S^m =$ 4/5, 2/15, or 8/15 for $m = 0$, 1, and 2, respectively; L(A) and L(B) are the $L(t)$ values at different sites. Usually, q_{zz} for deuterons is parallel to the chemical bond[5] and assumes the same value at A and B sites [q_{zz}(A) = q_{zz}(B)]. When considering the proton relaxation, the possibility of a change in the internuclear distance has to be taken into account. The dipolar coupling constants are $L(A) = \gamma_i\gamma_s\hbar R_{is}{}^{-3}(A)$ and $L(B) = \gamma_i\gamma_s\hbar R_{is}{}^{-3}(B)$, where R_{is}(A) and R_{is}(B) are the proton−proton distances at the A and B sites.

Spectral densities $J^m(\omega)$ in spin−lattice relaxation theories are Fourier transforms of the correlation functions of the fluctuating functions $F^m(t)$ of the dipole or quadrupole Hamiltonians:

$$J^m(\omega) = \int_{-\infty}^{+\infty}\langle F^m(t)\, F^m{}^*(t+\tau)\rangle\exp(-i\omega\tau)\,d\tau \quad (18)$$

Thus, the spectral density function of the complex motion composed of the classical and tunneling jumps between the two equilibrium positions A and B and the classical jumps between two other equilibrium positions is

$$J_{is(qcc)}^m(\omega) = \frac{S^m}{C_1 + C_2}\left\{\left(1 - \frac{3}{4}\sin^2\Theta_{lib}\right)\left[C_1C_2\left(\frac{2\tau_{\upsilon x}^{ov}}{1 + (\omega\tau_{\upsilon x}^{ov})^2} + \frac{2\tau_{\upsilon x}^{tu}}{1 + (\omega\tau_{\upsilon x}^{tu})^2}\right) + (C_2)^2\frac{2\tau_{\upsilon x}^{ovtu}}{1 + (\omega\tau_{\upsilon x}^{ovtu})^2}\right] + \frac{3}{4}\sin^2\Theta_{lib}\left[(C_1)^2\frac{2\tau^{lib}}{1 + (\omega\tau^{lib})^2} + C_1C_2\left(\frac{2\tau_{\upsilon x}^{ovlib}}{1 + (\omega\tau_{\upsilon x}^{ovlib})^2} + \frac{2\tau_{\upsilon x}^{tulib}}{1 + (\omega\tau_{\upsilon x}^{tulib})^2}\right) + (C_2)^2\frac{2\tau_{\upsilon x}^{ovtulib}}{1 + (\omega\tau_{\upsilon x}^{ovtulib})^2}\right]\right\} \quad (19)$$

where

$$\frac{1}{\tau_{\upsilon x}^{ovlib}} = \frac{1}{\tau_{\upsilon x}^{ov}} + \frac{1}{\tau^{lib}} \quad (20)$$

$$\frac{1}{\tau_{\nu x}^{\text{tulib}}} = \frac{1}{\tau_{\nu x}^{\text{tu}}} + \frac{1}{\tau^{\text{lib}}} \tag{21}$$

and

$$\frac{1}{\tau_{\nu x}^{\text{ovtulib}}} = \frac{1}{\tau_{\nu x}^{\text{ov}}} + \frac{1}{\tau_{\nu x}^{\text{tu}}} + \frac{1}{t^{\text{lib}}} \tag{22}$$

When $\tau_{\nu x}^{\text{tu}} \rightarrow \infty$, eq 19 simplifies to

$$J_{is(qcc)}^{m}(\omega) = S^{m}\left[C_1 \frac{3}{4}\sin^2\Theta_{\text{lib}} \frac{2\tau^{\text{lib}}}{1+(\omega\tau^{\text{lib}})^2} + C_2\left(1-\frac{3}{4}\sin^2\Theta_{\text{lib}}\right) \times \frac{2t_{\nu x}^{\text{ov}}}{1+(\omega\tau_{\nu x}^{\text{ov}})^2} + C_2\frac{3}{4}\sin^2\Theta_{\text{lib}} \frac{2\tau_{\nu x}^{\text{ovlib}}}{1+(\omega\tau_{\nu x}^{\text{ovlib}})^2}\right] \tag{23}$$

which is the theoretical value of spectral density for the complex motion consisting of two classical motions between two sites of potential energy minimums.[29,30]

When $\tau_{\nu x}^{\text{tu}} \rightarrow \infty$ and $\tau^{\text{lib}} \rightarrow \infty$, eq 19 simplifies to

$$J_{is(qcc)}^{m}(\omega) = S^{m}C_2 \frac{2\tau_{\nu x}^{\text{ov}}}{1+(\omega\tau_{\nu x}^{\text{ov}})^2} \tag{24}$$

which is the equation obtained by Nagaoka et al.[18] as well as Andrew and Latanowicz[31] for the classical hopping in a double potential.

3. Experiment

2,5-Dinitrobenzoic acid was purchased from Aldrich. By repeated recrystallization in ethanol-OD, it was specifically deuterated in the hydroxyl group. The deuteration was approximately 97%. Powder samples were used for measurements. The samples were degassed under 10^{-5} Torr and sealed under a vacuum in glass ampoules.

Proton T_1 values were measured on a Bruker SXP 4/100 pulse spectrometer at 24.7 MHz by a conventional saturation recovery technique with a saturation sequence of 15 90° pulses, each followed by a 4 ms delay.

Proton $T_{1\rho}$ values were measured with a 24.7 MHz Bruker SXP 4/100 pulse spectrometer. The quantity $T_{1\rho}$ was determined by locking the signal after a 90° pulse and observing the subsequent signal intensity as a function of the field pulse duration. The magnetic radiofrequency field $B_1 = 9$ G was applied.

Deuterium T_1 relaxation measurements were performed at a Larmor frequency of 55.2 MHz. An aperiodic saturation pulse sequence was employed to initially destroy the z magnetization M_z, and the subsequent buildup of M_z was monitored with a $90°_x - t - 90°_y$ echo sequence. A measure of M_z was the height of the echo.

The temperature of the specimen was kept constant automatically during a measurement by an Oxford temperature controller to an accuracy of 0.1 K.

4. Results and Discussion

A. Proton Relaxation. The experimental temperature dependencies of protons T_1 (24.7 MHz, □) and $T_{1\rho}$ ($B_1 = 9$ G, △) are given in Figure 2 together with that of T_1 at 55.2 MHz (○, published previously).[1] Fits of eq 6 together with those of eqs 19, 1, 3, and 5 and the known structural data for R_{is}(A), R_{is}(B), and the angles Θ_{AB} to the experimental T_1 and $T_{1\rho}$ data are represented in Figure 2 by solid lines. The crystal structure of 2,5-DNBA has been solved by Grabowski and Krygowski.[22] The obtained best-fit parameters E_{AB}, Δ, $(\tau_0^{\text{ov}})_{\nu 0}$, $(\tau_0^{\text{tu}})_{\nu 0}$, E_{lib}, τ_0^{lib}, and Θ_{lib} are listed in Table 1. The best-fit parameters Δ and $(\tau_0^{\text{tu}})_{\nu 0}$ were obtained from T_1 temperature dependencies, while the best-fit parameters E_{lib}, τ_0^{lib}, and Θ_{lib} were obtained from $T_{1\rho}$ temperature dependence only. The values E_{AB} and $(\tau_0^{\text{ov}})_{\nu 0}$ fit the experimental data of $T_{1\rho}$ as well as T_1. The dashed lines in Figure 2 show the fits of eqs 6 and 23 to the experimental data. Equations 19 and 23 differ by the taking into consideration the tunneling motion. It is clearly visible that low-temperature minimum $T_{1\rho}$ can be assigned to the classical motion.

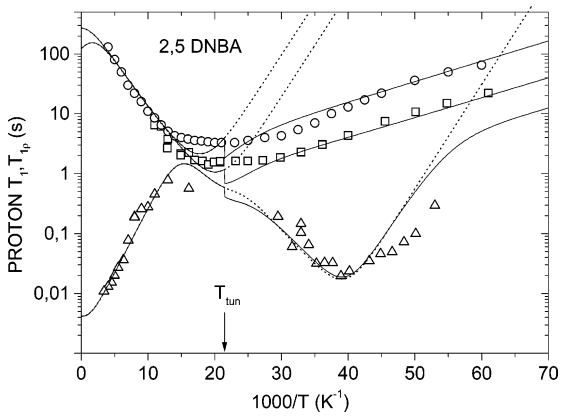

Figure 2. Temperature dependencies of the proton T_1 (○ = 55.2 MHz) and (□ = 24.7 MHz) and $T_{1\rho}$ [(Δ − (B_1 = 9 G, $\omega_I = 2\pi \times 2.47$ MHz)]) for 2,5-DNBA. Solid lines represent the best fit of eqs 6 and 19 together with eqs 1, 3, and 5 to the experimental data. Dotted lines represent the best fit of experimental data when eq 23 is applied. The arrow shows the temperature of cessation of proton tunneling jumps (T_{tun} = 46.5 K).

Thus, the possibility of determination of the correlation times $\tau_{\nu x}^{\text{ov}}$ and τ^{lib} from the temperature dependence of T_1 depends not on the temperature range but on the resonance frequency at which the measurements were performed. The slopes of $T_{1\rho}$ from both sides of the minimum are higher than the slope of T_1 in the same temperature regime. This indicates that $T_{1\rho}$ is a result of classical hopping, while T_1 is mainly a result of incoherent tunneling at these temperatures. Therefore, it can be concluded that $T_{1\rho}$ in the low-temperature regime is governed by classical motion, while T_1 in the same temperature regime is governed by incoherent tunneling. Thus, the $T_{1\rho}$ relaxation time in the rotating frame is a convenient experiment to detect the rate of classical motion, $1/\tau_{\nu x}^{\text{ov}}$, at low temperatures.

The $T_{1\rho}$ minimum revealed by experimental points at the highest temperatures (Figure 2), but below the melting point, corresponds to the maximum of the function $2\tau^{\text{lib}}/[1 + (2\omega_1\tau^{\text{lib}})^2]$. The corresponding minimum of T_1 is a result of the maximums of the functions $2\tau^{\text{lib}}/[1 + (\omega_I\tau^{\text{lib}})^2]$ and $2\tau^{\text{lib}}/[1 + (2\omega_I\tau^{\text{lib}})^2]$. Such a minimum is not reached in measurements T_1 (55.2 MHz) or T_1 (24.7 MHz) below the melting point. Therefore, $T_{1\rho}$ measurements only detect the librations of the whole molecule between two equilibrium positions distanced by the angle Θ_{lib}. The best fit estimated for the value of Θ_{lib} is 30°.

The small discontinuities in the temperature dependencies in Figure 2 follow from the fact of inserting eq 3 into eq 19. When $C_pT > E_{\text{AB}}$, the correlation time $\tau_{\nu x}^{\text{tu}}$ is eliminated from the equations for the spectral density (eq 19). Therefore, spectral density follows eq 23 above the characteristic temperature T_{tun} where $C_pT_{\text{tun}} = E_{\text{AB}}$. The potential barrier estimated from the

TABLE 1: The Best-Fit Parameters Obtained from the Proton T_1 and $T_{1\rho}$ and Deuteron T_1 (Deuterated Hydroxyl Group) of 2,5-DNBA

	E_{AB} kJ/mol	(Δ) kJ/mol	E_{lib} kJ/mol	$(\tau_0^{ov})_{\upsilon 0}$ s	$(\tau_0^{tu})_{\upsilon 0}$ s	τ_0^{lib} s	Θ_{lib} deg
proton	3.3	0.63	4.2	5.9×10^{-12}	3×10^{-9}	2×10^{-6}	30
deuteron	6.3	0.42		3.3×10^{-11}	9×10^{-8}		

high-temperature side of the temperature dependence of T_1 is 3.35 kJ/mol. The excellent fit of eqs 6 and 19 (Figure 2) to the experimental data is obtained when the temperature T_{tun} is assumed to be approximately 46.5 K. This value is shown by the arrow in Figure 2. Therefore, the value of C_p is 72 J/mol/K. The value of C_p in solids is temperature-dependent. The knowledge of the accuracy of C_p determination is important in the temperature just below the T_{tun} temperature. For small values of T ($C_pT \ll E_{ov}$), the values τ^{tu} (eq 3) are mainly determined by the value of E_{ov}:

$$\tau^{tu} \approx \tau_0^{tu} \exp(B\sqrt{E_{ov}}) \tag{25}$$

Therefore, $C_p = 72$ J/mol/K is the value of the molar heat capacity of 2,5-DNBA just near the temperature 46.5 K.

It is clear that the values of $n_{\upsilon 1}J^m(\omega,\tau_{\upsilon 1}^{ov},t_{\upsilon 1}^{tu})$ are relatively small for proton transfer because there is virtually no difference between the calculated spin−lattice relaxation times according to eq 6 and the equation

$$\frac{1}{(T_1)} = \frac{1}{N}\sum_{i=1}^{N}\sum_{s=1}^{N} n_{\upsilon 0}\frac{1}{(T_1^{is})_{\upsilon 0}} \tag{26}$$

B. Deuteron Relaxation. The experimental deuteron relaxation time T_1 (55.2 MHz) as a function of the temperature for a powdered sample of 2,5-DNBA is presented in Figure 3 together with the theoretical best-fit plots. The value $L(A) = L(B) = qcc = 175$ kHz, used in these fits, was estimated from the expression[32]

$$qcc = (442.7 - 4882r^{-3})\ \text{kHz} \tag{27}$$

where r is the O···O distance in angstroms, estimated to be 2.63 Å.[22] The asymmetry parameter η has been assumed to be equal to zero. The angle θ_{AB} between the orientations of the principal component of the electric field gradient tensor q_{zz}, assumed to be along the O−D chemical bond, was estimated from the known structure to be 7°.[22]

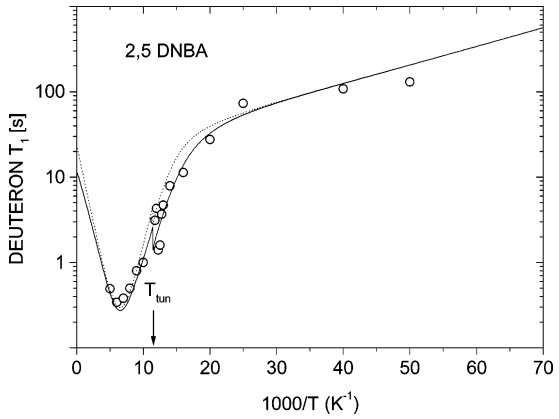

Figure 3. Experimental deuteron T_1 (55.2 MHz) for 2,5-DNBA with deuterated hydroxyl group as a function of the temperature. Solid lines represent the best fit of eqs 28 and 19 together with eqs 1, 3, and 5 to the data. The dotted lines represent the best fit when the first term in eq 28 is applied. The arrow shows the temperature of cessation of deuteron tunneling jumps ($T_{tun} = 87.3$ K).

We performed two kinds of fits. One of them (solid line) weighted in the deuteron population average value of deuteron T_1, that is,

$$\frac{1}{(T_1^{deut})} = n_{\upsilon 0}\frac{1}{(T_1^{deut})_{\upsilon 0}} + n_{\upsilon 1}\frac{1}{(T_1^{deut})_{\upsilon 1}} \tag{28}$$

where $1/(T_1^{deut})_{\upsilon x}$ is given by eqs 11 and 19 and the other (dotted line) with the first term of eq 28. The fit presented by the dotted line deviates noticeably from the experimental points, while the solid lines fit the experimental data satisfactory. The difference between the dotted and solid lines reveals the temperature regime where the proton transfer of molecules being in the first excited vibrational state contributes to the deuteron relaxation of 2,5-DNBA. Thus, a contribution to NMR spin−lattice relaxation due to proton transfer in excited vibrational states is negligible for fast proton transfer but is significant for slow deuteron transfer.

The best-fit parameters are listed in Table 1. As a result of the isotope effect, deuteron-transfer parameters differ from those of protons. Since a deuteron is heavier than a proton, it moves slower in the hydrogen bond. The potential barrier E_{AB} for the interconversion of the A ↔ B tautomers is higher for deuterons than for protons.

5. Correlation Times

The best-fit parameters E_{AB}, Δ, $(\tau_0^{ov})_{\upsilon 0}$, $(\tau_0^{tu})_{\upsilon 0}$, E_{lib}, and τ_0^{lib} given in Table 1 can be used to calculate the theoretical temperature dependence of the proton and deuteron correlation times. The temperature dependencies of the correlation times $(\tau^{ov})_{\upsilon 0}$, τ^{lib}, and $(\tau^{tu})_{\upsilon 0}$ obtained from fits to the dependencies of T_1 (55.2 and 24.7 MHz) and $T_{1\rho}$ ($B_1 = 9$G) are shown in Figure 4 as solid lines. The points show the values of $(\tau^{ov})_{\upsilon 0}$ and $(\tau^{tu})_{\upsilon 0}$ obtained from the particular experimental data [∇ and $\Delta = T_1$ (24.7 MHz), ○ and □ $= T_1$ (55.2 MHz), and × and + $= T_{1\rho}$ ($B_1 = 9$G)]. The proton correlation times are given in Figure 4a, while the deuteron correlation times are given in Figure 4b. The plot of $\ln[(\tau^{tu})_{\upsilon 0}]$ as a function of $(1000/T)$ reveals the temperature T_{tun} shown in Figure 4 by the arrow. It is visible that at this temperature the value of correlation time $(\tau^{tu})_{\upsilon 0}$ is comparable to the value of $(\tau^{ov})_{\upsilon 0}$. The plot of $\ln[(\tau^{tu})_{\upsilon 0}]$ as a function of $(1000/T)$ deviates from the almost linear dependence at temperatures below T_{tun}. This effect follows from the specific temperature dependence of τ^{tu}, in accordance with eq 3. The temperature T_{tun} is the highest temperature for $(\tau^{tu})_{\upsilon 0}$ and $(\tau^{tu})_{\upsilon 1}$ temperature dependence.

As predicted by eqs 1, 3, and 5, the correlation times of the classical motions τ^{ov} and τ^{lib} exist in a wide temperature range while the tunneling correlation time τ^{tu} exists only in low temperatures up to the temperature $T_{tun} = E_{ov}/C_p$. Below the T_{tun} temperature, the thermal energy of molecules (C_pT) is lower than the activation energy. This temperature seems to be also the point where correlation times of tunneling and classical motion are of comparable value.

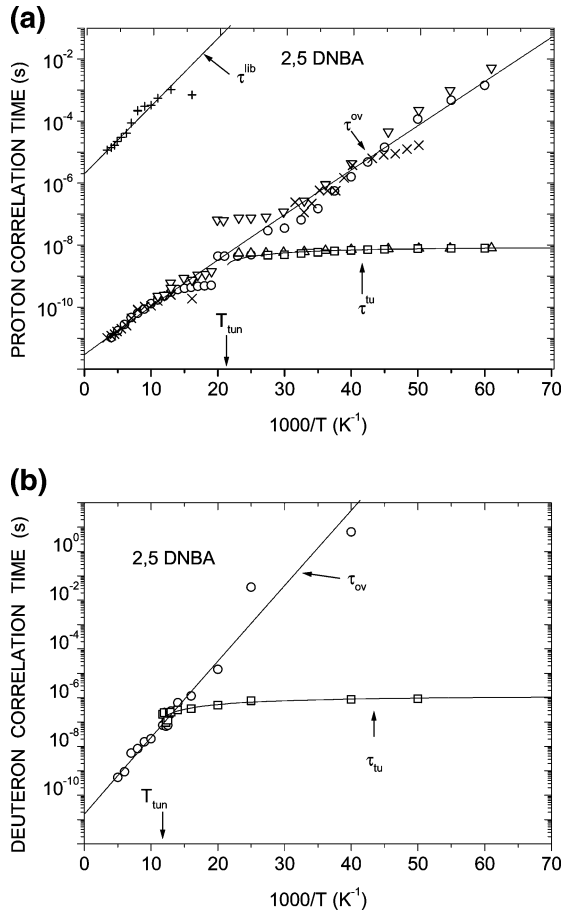

Figure 4. Proton (a) and deuteron (b) correlation times as a function of the temperature for 2,5-DNBA. Points refer to the experimental values $(\tau^{ov})_{i0}$, $(\tau^{tu})_{i0}$, and τ^{lib} obtained from the proton and deuteron T_1 temperature dependencies. Proton T_1 (55.2 MHz) = ○, □; proton T_1 (24.7 MHz) −▽, △; proton $T_{1\rho}$ (B_1 = 9 G, ν_I = 24.7 MHz) − ×, +. Lines refer to the calculated correlation times obtained from eqs 1, 3, and 5 and best-fit parameters given in Table 1.

6. Comparison to Other Relaxation Theories

Instead of the spectral density given by eq 19, the following equation has been used in the literature as an approximation of the total spectral density due to classical motion and incoherent tunneling:[1−13]

$$J^{m}_{is(qcc)}(\omega) = S^{m}C_2 \frac{2\tau^{\text{total}}}{1+(\omega\tau^{\text{total}})^2} \qquad (29)$$

The correlation time τ^{total} as a function of the temperature is usually approximated by a biexponential dependence[6] whose first term is the Arrhenius-like dependence, and the second describes the deviations from the Arrhenius law. In a number of papers, the second term in the formula for t^{total} is as shown below

$$\frac{1}{\tau^{\text{total}}} = \frac{1}{\tau^{\text{ov}}} + \frac{1}{\tau^{\text{tu}}} \qquad (30)$$

where τ^{ov} and τ^{tu} are determined by the Arrhenius and Skinner−Trommsdorff[2] dependencies.

Differences between two models (eqs 19 and 29) are noticeable in the calculations of spin−lattice relaxation rates for high and low resonance frequencies.[33] In fact, it was impossible to obtain an acceptable fit to both proton T_1 (ω_I = $2\pi \times$ 55.2 MHz, $\omega_I = 2\pi \times$ 24.7 MHz) and $T_{1\rho}$ (B_1 = 9 G), obtained for 2,5-DNBA data, by employing eq 29 (Figure 5).

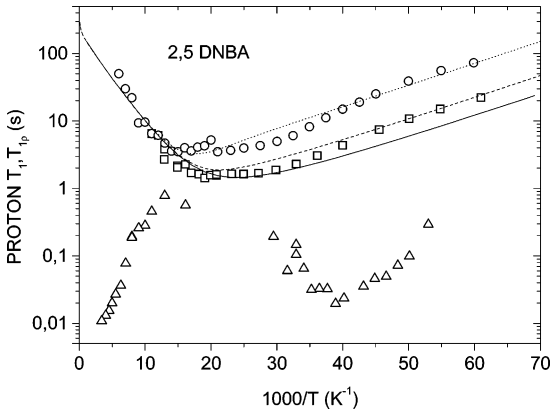

Figure 5. The temperature dependence of proton T_1 (○ − 55.2 MHz, □ − 24. 7 MHz) and $T_{1\rho}$ [(Δ − (B_1 = 9 G, $\omega_I = 2\pi \times$ 24.7 MHz)] for 2,5-DNBA. The dotted line represents the best fit of eqs 6, 9, 10, 29, and 30 to the experimental data T_1 (55. 2 MHz). The Skinner−Trommsdorff formula[2] was employed for τ^{tu}. The best-fit parameters obtained from the T_1 (55. 2 MHz) temperature dependence were used to plot the T_1 (dashed line − 24. 7 MHz) and $T_{1\rho}$ [solid line − (B_1 = 9 G)] versus the temperature.

7. Conclusions

The correlation time for tunneling jumps can be described explicitly by a formula obtained directly from Schrödinger's equation. The low temperature of the beginning of the tunneling motion, T_{tun}, predicted by this equation, is approximately 46.5 K for proton transfer and 87.3 K for deuteron transfer in 2,5-DNBA dimer. These temperatures point to the temperatures where the thermal energy C_pT equals the activation energy. Below T_{tun}, the temperature begins the tunnel pathway for proton transfer.

The equations derived in this paper for the total spectral density of complex motion (classical and tunneling jumps of a hydrogen-bonded proton, two-site hopping of the whole dimer) fit well the T_1 and $T_{1\rho}$ experimental data.

Employing the model with a single correlation time for proton transfer is not possible to fit both the $T_{1\rho}$ and T_1 experimental data.

References and Notes

(1) Medycki, W.; Idziak, S. *Mol. Phys.* **1995**, *86*, 257.
(2) Skinner, J. L.; Trommsdorff, H. P. *J. Chem. Phys.* **1988**, *89*, 897.
(3) Meyer, R.; Ernst, R. R. *J. Chem Phys.* **1990**, *93*, 5518.
(4) Stöckli, A.; Meier, B. H.; Kreis, R.; Meyer, R.; Ernst, R. R. *J. Chem. Phys.* **1990**, *93*, 1502.
(5) Heuer, A.; Haeberlen, U. *J. Chem. Phys.* **1991**, *95*, 4201.
(6) Hoelger, Ch.; Werhle, B.; Benedict, H.; Limbach, H. H. *J. Phys. Chem.* **1994**, *98*, 843.
(7) Horsewill, A. J.; Ikram, A.; Tomash, I. B. *Mol. Phys.* **1995**, *84*, 1257.
(8) Brougham, D. F.; Horsewill, A. J.; Jenkinson, R. I. *Chem. Phys. Lett.* **1997**, *272*, 69.
(9) Horsewill, A. J.; Brougham, D. F.; Jenkinson, R. I.; McGloin, C. J.; Trommsdorff, H. P.; Johnson, M. R. *Ber. Bunsen.-Ges. Phys. Chem.* **1998**, *102*, 317.
(10) Medycki, W.; Reynhardt, E. C.; Latanowicz, L. *Mol. Phys.* **1998**, *93*, 323.
(11) Horsewill, A. J.; McGloin, C. J.; Trommsdorff, H. P.; Johnson, M. R. *Chem. Phys.* **2003**, *291*, 41.
(12) Jenkinson, R. I.; Ikram, A.; Horsewill, A. J.; Trommsdorff, H. P. *Chem. Phys.* **2003**, *294*, 95.
(13) Wu, W.; Noble, D. L.; Horsewill, A. J. *Chem. Phys. Lett.* **2005**, *402*, 519.
(14) Reynhardt, E. C.; Latanowicz, L. *J. Magn. Reson.* **1998**, *130*, 195.
(15) Latanowicz, L.; Reynhardt, E. C. *Chem. Phys. Lett.* **2001**, *341*, 561.

(16) Latanowicz, L.; Reynhardt, E. C. Boguszynska, J. *THEOCHEM* **2004**, *710*, 111.
(17) Woessner, D. E. *J. Chem. Phys.* **1962**, *36*, 1.
(18) Nagaoka, S.; Terao, T.; Imashiro, F.; Saika, A.; Hirota, N.; Hayashi, S. *J. Chem. Phys.* **1983**, *79*, 4694.
(19) Latanowicz, L. *J. Phys. Chem. A* **2004**, *108*, 11172.
(20) Latanowicz, L. *Concepts Magn. Reson. Part A* **2005**, *27A*, 38.
(21) Latanowicz, L.; Medycki, W.; Jakubas R. *J. Phys. Chem*. **2005**, *109*, 3097.
(22) Grabowski, S. J.; Krygowski, T. M. *Acta Crystallogr., Sect. C* **1985**, *41*, 224.
(23) Abragam, A. *The Principles of Nuclear Magnetism*; Oxford University Pres: Oxford, U. K., 1961.
(24) Redfield, A. G. *Phys. Rev*. **1955**, *98*, 1787.
(25) Mehring, M. *Principles of High Resolution NMR in Solids*; Springer: Berlin, 1983.
(26) Woessner, D. E.; Snowden, B. S.; Meyer, G. H. *J. Chem. Phys.* **1969**, *50*, 719.
(27) Spiess, H. W. *NMR Basis Principles and Progress*; Springer: Berlin, 1978; Vol. 15, pp 55−214.
(28) Hentschel, R.; Silescu, H.; Spiess, H. W. *Polymer* **1981**, *22*, 1516.
(29) Latanowicz, L.; Reynhardt, E. C. *J. Magn. Reson., Ser. A* **1996**, *121*, 23.
(30) Latanowicz, L.; Reynhardt, E. C. *Mol. Phys.* **1997**, *90*, 107.
(31) Andrew, E. R.; Latanowicz, L. *J. Magn. Reson*. **1986**, *68*, 232.
(32) Hunt, M. J.; Mackay, A. L. *J. Magn. Reson*. **1974**, *15*, 402.
(33) Latanowicz, L.; Reynhardt, E. C. *Chem. Phys. Lett.* **2007**, *433*, 444.